



UNIVERSITY OF LEEDS

This is a repository copy of *Ag@Ni Core-Shell Nanowire Network for Robust Transparent Electrodes Against Oxidation and Sulfurization*.

White Rose Research Online URL for this paper:
<http://eprints.whiterose.ac.uk/164287/>

Version: Accepted Version

Article:

Eom, H, Lee, J orcid.org/0000-0002-7768-7061, Pichitpajongkit, A et al. (5 more authors) (2014) *Ag@Ni Core-Shell Nanowire Network for Robust Transparent Electrodes Against Oxidation and Sulfurization*. *Small*, 10 (20). pp. 4171-4181. ISSN 1613-6810

<https://doi.org/10.1002/sml.201400992>

© 2014 WILEY-VCH Verlag GmbH & Co. KGaA, Weinheim. This is the peer reviewed version of the following article: Eom, H., Lee, J., Pichitpajongkit, A., Amjadi, M., Jeong, J.-H., Lee, E., Lee, J.-Y. and Park, I. (2014), *Ag@Ni Core-Shell Nanowire Network for Robust Transparent Electrodes Against Oxidation and Sulfurization*. *Small*, 10: 4171-4181. , which has been published in final form at <https://doi.org/10.1002/sml.201400992>. This article may be used for non-commercial purposes in accordance with Wiley Terms and Conditions for Use of Self-Archived Versions.

Reuse

Items deposited in White Rose Research Online are protected by copyright, with all rights reserved unless indicated otherwise. They may be downloaded and/or printed for private study, or other acts as permitted by national copyright laws. The publisher or other rights holders may allow further reproduction and re-use of the full text version. This is indicated by the licence information on the White Rose Research Online record for the item.

Takedown

If you consider content in White Rose Research Online to be in breach of UK law, please notify us by emailing eprints@whiterose.ac.uk including the URL of the record and the reason for the withdrawal request.



eprints@whiterose.ac.uk
<https://eprints.whiterose.ac.uk/>

1
2 **Ag@Ni core-shell nanowire network for robust transparent electrodes against oxidation**
3 **and sulfurization**
4
5
6

7 *Hyeonjin Eom, Jaemin Lee, Aekachan Pichitpajongkit, Morteza Amjadi, Jun-Ho Jeong,*
8 *Eungsug Lee, Jung-Yong Lee and Inkyu Park**
9

10
11
12 H. Eom

13 Department of Mechanical Engineering
14 291 Daehak-ro, Yuseong-gu, Daejeon 305-701, Republic of Korea
15 Korea Advanced Institute of Science and Technology (KAIST),
16 Department of Nano Manufacturing Technology
17 156, Gajeongbuk-Ro, Yuseong-Gu, Daejeon 305-343, Republic of Korea
18 Korea Institute of Machinery & Materials (KIMM)
19
20
21

22
23 [*] Prof. I. Park

24 Department of Mechanical Engineering and KI for the NanoCentury (KINC)
25 291 Daehak-ro, Yuseong-gu, Daejeon 305-701, Republic of Korea
26 Korea Advanced Institute of Science and Technology (KAIST)
27 inkyu@kaist.ac.kr
28
29

30 J. Lee, J.Y. Lee

31 Graduate School of Energy, Environment, Water, and Sustainability (EEWS), and KI for the
32 NanoCentury (KINC)
33 291 Daehak-ro, Yuseong-gu, Daejeon 305-701, Republic of Korea
34 Korea Advanced Institute of Science and Technology (KAIST)
35
36

37 A. Pichitpajongkit

38 Department of Mechanical Engineering
39 291 Daehak-ro, Yuseong-gu, Daejeon 305-701, Republic of Korea
40 Korea Advanced Institute of Science and Technology (KAIST)
41
42

43 M. Amjadi

44 Department of Mechanical Engineering, KI for the NanoCentury (KINC)
45 291 Daehak-ro, Yuseong-gu, Daejeon 305-701, Republic of Korea
46 Korea Advanced Institute of Science and Technology (KAIST)
47
48

49 E. Lee, J.H. Jeong

50 Department of Nano Manufacturing Technology
51 156, Gajeongbuk-Ro, Yuseong-Gu, Daejeon 305-343, Republic of Korea
52 Korea Institute of Machinery & Materials (KIMM)
53
54
55

56
57 Keywords:

58
59 Transparent electrode, core-shell nanostructure, electrodeposition, anti-oxidation and anti-
60 sulfurization
61
62

Abstract:

Silver nanowire (Ag NW) based transparent electrode is inherently unstable to moist and chemically reactive environment. We report a remarkable stability improvement of the Ag NW network film against oxidizing and sulfurizing environment by local electrodeposition of Ni along Ag NWs. The optical transmittance and electrical resistance of the Ni deposited Ag NW network film can be easily controlled by adjusting the morphology and thickness of the Ni shell layer. The electrical conductivity of the Ag NW network film is increased by the Ni coating via welding between Ag NWs as well as additional conductive area for the electron transport by electrodeposited Ni layer. Moreover, the chemical resistance of Ag NWs against oxidation and sulfurization can be dramatically enhanced by the Ni shell layer electrodeposited along the Ag NWs, which provides the physical barrier against chemical reaction and diffusion as well as the cathodic protection from galvanic corrosion.

1 **1. Introduction**

2
3 Transparent conductive electrodes (TCEs) have been investigated for numerous
4 applications including mobile display, photovoltaic energy generation, and liquid crystal
5 display applications.^[1-3] Indium tin oxide (ITO) is the most widely used material for
6 transparent electrodes due to its high electrical conductivity and transparency in the visible
7 range.^[4] However, ITO is not suitable for flexible devices due to its poor mechanical
8 flexibility and brittleness. The mechanical robustness of bare ITO films could be increased by
9 the formation of multiple ITO-polymer composite layers.^[5] Nevertheless, multi-layered ITO
10 film was mechanically and electrically broken under the strain of $\epsilon = 0.017$, which is lower
11 than the requirement for flexible displays.^[6] As alternatives to the ITO-polymer composite,
12 solution-processible TCEs such as carbon nanotubes, graphene and metal mesh films have
13 been intensively studied due to their superior mechanical characteristics as compared to the
14 oxide based TCEs.^[7-9]

15
16 Recently, silver nanowire (Ag NW) network structure has been studied as a promising
17 alternative transparent electrode with several advantages such as high transparency, good
18 electrical conductivity, and mechanical flexibility.^[10] The synthesis of Ag NWs by the polyol
19 reaction^[11-13] is very simple and high throughput for the large scale production of Ag NWs.^[14]
20 The transparent Ag NW network film can be obtained by spin-coating,^[15] spray coating^[16]
21 and bar coating processes^[17] due to facile formation of stable liquid phase suspension of NWs.

22
23 Despite the abovementioned advantages of Ag NWs, they cannot be used for a long term
24 period due to their chemical instability. The electrical conductivity of Ag NWs can be easily
25 degraded by the chemical instabilities such as oxidation and sulfurization.^[18, 19] For example,
26 the exposed Ag NW network film under electrical current flow can be easily oxidized and
27 sulfurized by oxygen and sulfur from the air.^[18] The Ag:Mg cathode of organic light emitting
28 devices (OLED) shows the nonemissive spots at Ag:Mg cathode-organic interface owing to
29 the gas evolution from the galvanic corrosion of the Mg/Ag couple.^[20] Even if the Ag NW

1 film is embedded within the device or protected by the polymer passivation layer, it can still
 2
 3 be attacked though small voids or cracks.^[21] Moreover, the polymer-coated Ag NW network
 4
 5 films have a possibility to react with sulfur-containing gases since many polymers are
 6
 7 permeable to gaseous molecules.^[22] The chemical stability of the metal NWs has been
 8
 9 recently studied for the improvement of their durability as conductive metal electrodes. For
 10
 11 example, the AgNW network film protected by graphene oxide (GO) sheets shows better
 12
 13 chemical stability in the air.^[23] Also, Ag NW network film buried into the surface of the
 14
 15 polymer substrate exhibited better sulfurization-resistivity than the conventional Ag NW
 16
 17 network films that are entirely exposed to the ambient environment.^[24] It took 1 minute for
 18
 19 the buried AgNW network film to be completely nonconductive whereas only 3 seconds were
 20
 21 required to completely disconnect the fully exposed Ag NW network under sulfurization
 22
 23 condition (5 wt% Na₂S solution).^[24] The cupronickel (CuNi) NW network was utilized as an
 24
 25 alternative material for transparent electrodes and showed good anti-oxidation property due to
 26
 27 the anti-corrosion characteristics of Ni alloy in the moist condition.^[25] However, the CuNi
 28
 29 NW network provides higher electrical resistivity ($\rho = 1.33 \times 10^{-7} \sim 2.34 \times 10^{-7} \Omega \cdot \text{m}$) than those
 30
 31 of both Ag and Cu NW networks ($\rho_{\text{AgNW}} = 1.29 \times 10^{-7} \Omega \cdot \text{m}$ ^[26] and $\rho_{\text{CuNW}} = 7.51 \times 10^{-}$
 32
 33 $8 \Omega \cdot \text{m}$ ^[25]).

34
 35
 36
 37
 38
 39
 40
 41
 42 Herein, we introduce a novel method to improve the chemical resistance of the Ag NW
 43
 44 network film based electrode by forming the Ni protective shell on the surface of the Ag NWs
 45
 46 without degradation of their electrical conductivity. The Ni coated Ag NW network film is
 47
 48 prepared by the local electrodeposition, and its superior anti-oxidation and anti-sulfurization
 49
 50 characteristics are investigated in this work. **Figure 1a** shows the mechanisms of the anti-
 51
 52 oxidation and anti-sulfurization of Ni coated Ag NW network film under oxygen species (O₂
 53
 54 and OH) and sulfur(S)-containing environments. As shown in the inset of Figure 1a, the Ni
 55
 56 shell layer deposited on Ag NWs acts as an electron-donor to Ag NWs as well as a physical
 57
 58
 59
 60
 61
 62
 63
 64
 65

1 barrier against the reaction or diffusion of O_2 and OH^- so that the oxidation of Ag NWs in
2
3 oxygen environment is prevented. In the case of the sulfur-containing environment, the Ni
4
5 shell layer on the exposed area of the Ag NW network film protects the Ag NW network film
6
7 from sulfurization by similar mechanisms.
8
9

10 Ag NWs were synthesized by the polyol method.^[14] The synthesis processes are explained
11
12 in the experimental section with details. Figure panels 1b-f show the schematic of the Ni
13
14 coated Ag NW network film on the flexible polymer substrate (polydimethylsiloxane (PDMS)
15
16 film in this study). First, the Ag NW network film is formed on the donor substrate
17
18 (polyimide (PI) film in this study) by spray coating process (Figure 1b). Then, the Ag NW
19
20 network film is pressed by a PDMS block to attach Ag NWs firmly onto the PI substrate and
21
22 to strengthen the bonding between Ag NWs so that the soaking of the liquid PDMS into the
23
24 gap between Ag NWs can be prevented. Then, the liquid PDMS is poured on the Ag NW
25
26 network film and cured in a convection oven at 100 °C for 4 hours, and the Ag NW network
27
28 film partially embedded on the PDMS layer is peeled off from the PI film (Figure 1c-d).
29
30 Partial embedding formed the robust Ag NW-PDMS composite thin film on the PDMS layer
31
32 and prevented the Ag NWs from being detached during the electrodeposition process. Finally,
33
34 the Ni layer is electrodeposited on the exposed surface of the Ag NW network film (see
35
36 Figure panels 1e-f) by using a 3-electrode system in a Ni electrodeposition bath for various
37
38 time periods. (Detail of electrodeposition process is explained in the experimental section) The
39
40 thickness of the Ni layer can be controlled by the electrodeposition period (Figure 1f).
41
42
43
44
45
46
47
48
49
50

51 **2. Results and Discussion**

52 **Figure 2a** shows the surface morphologies of the Ag NW network film partially buried on
53
54 the surface of PDMS substrate. The average diameter and length of Ag NWs are 45.05 nm
55
56 (± 10.67 nm) and 15.93 μm ($\pm 2.43 \mu\text{m}$), respectively. The measured geometrical fill factor (FF)
57
58 of the buried Ag NWs on the surface of PDMS substrate is 23.39 %. As the figure shows, Ag
59
60
61
62
63
64
65

1 NWs are well connected with each other forming a percolation network. After the
 2
 3 electrodeposition of the Ni thin film on the exposed areas of the Ag NW network film for
 4
 5 various periods, different morphologies of the Ni nanostructures were observed on the surface
 6
 7 of the Ag NW network film, as shown in Figure panels 2 b-e. Table 1 illustrates the measured
 8
 9 diameters of Ni coated Ag NWs for different electrodeposition periods of 5, 20, 50 and 100
 10
 11 seconds. Hereafter, sample A, B, C and D refer to the Ag NWs coated with Ni for 5, 20, 50
 12
 13 and 100 seconds of electrodeposition, respectively. The electrodeposition rates of the Ni layer
 14
 15 on the Ag NW network film are calculated as 0.84 nm/sec, 1.36 nm/sec, 2.20 nm/sec and 2.33
 16
 17 nm/sec for the samples A, B, C and D, respectively. The increase of deposition rate is
 18
 19 presumably due to the increase of surface area and electrical current for the electrochemical
 20
 21 reaction. After a short Ni electrodeposition period (~5sec), it was difficult to visually observe
 22
 23 the formation of the Ni layer on the surface of the Ag NW network film (see Figure 2b).
 24
 25 However, we could estimate the deposited thickness of the Ni layer (2.62 nm) from the
 26
 27 electrical charge (~0.0046 C, Figure S2) by the electrodeposition process according to
 28
 29 Faraday's law^[27]. After 20 seconds of electrodeposition, discrete Ni nano-dot layers could be
 30
 31 observed on the surface of Ag NWs (Figure 2c). After the electrodeposition for 50 and 100
 32
 33 seconds, the deposition of dense Ni layers could be observed on the surface of Ag NWs
 34
 35 (Figure panels 2d and e). According to the electrical current-deposition time (i-t) curve of the
 36
 37 samples, almost equal currents are measured for different samples at the same
 38
 39 electrodeposition time, which verifies the repeatability of Ni electrodeposition process with
 40
 41 similar exposed area of the Ag NW network film (**Figure S1**). Therefore, we can assume that
 42
 43 the thickness of the deposited Ni layer can be controlled by the electrodeposition periods. ^[27]
 44
 45 The deposition thickness and shape of Ni layer can be also predicted by numerical simulation
 46
 47 based on Faraday's law and Butler-Volmer equation.^[27] (See Supporting Information for
 48
 49 details) Figure 2f shows a good agreement between simulated and measured diameters of
 50
 51
 52
 53
 54
 55
 56
 57
 58
 59
 60
 61
 62
 63
 64
 65

1 Ag@Ni core-shell NWs for different electrodeposition periods. Figure panels 2g-2i illustrate
 2 the evolution of the Ni layer thickness and current density at different electrodeposition
 3 periods (t=0, 20 and 100 seconds) for half-embedded Ag NW. The thickness of Ni layer
 4 gradually increases with longer electrodeposition periods. Also, the thickness of Ni layer is
 5 almost equal in all angular orientations due to the uniform distribution of electrolytic potential
 6 and current density (eg. -0.2021 V and 2.321 mA/m² at 20 seconds) around the Ag NW.
 7
 8 Similar tendency is found in the case of the Ni electrodeposition on the protruded Ag NW (i.e.
 9 5.21 area % embedded in the substrate). (See Figure S1) Therefore, the thickness and
 10 directional uniformity of the Ni coated layer can be easily controlled by the electrodeposition
 11 process.

12
 13 The sheet resistances of the Ni coated Ag NW network films are lower than that of the
 14 pristine Ag NW network film. The high electrical resistance of Ag NW network film is
 15 caused by high junction resistance between Ag NWs.^[6] The sheet resistance of the Ni coated
 16 Ag NW network film is gradually decreased by the increase of the Ni electrodeposition period
 17 (**Figure 3a**). For example, the Ni deposited Ag NW network films after a long
 18 electrodeposition period (i.e. 100 s) possesses a very low sheet resistance (9.92(±5.42) Ω/sq)
 19 as compared with that of the pristine Ag NW network film (31.07(±3.56) Ω/sq). Increase of
 20 the conductivity could be due to the additional contribution of the outer Ni shell layer to the
 21 electrical conductance as well as bonding improvement between Ag NWs via welding effect
 22 at the NW junctions. As shown in Figure 2, the FF of Ag NW is increased by electrodeposited
 23 Ni layer (23.39, 23.99, 29.34, 34.16 and 66.32% for pristine Ag NW, sample A, B, C and D,
 24 respectively) which represents enlargement of the current-carrying area. It should be noted
 25 that the Ni shell layer was not electrodeposited onto some Ag NWs that were fully embedded
 26 into the substrate or electrically disconnected from percolation network. However, the

1 electrodeposited Ni layer provided welding between loosely connected or separated Ag NWs
2
3 as shown Figure panels 2d and e.
4

5 The transmittance spectra of the pristine Ag NW network film and Ni coated Ag NW
6 network film were measured to quantify their optical characteristics. In order to quantify their
7 transmittance without the substrate effect, we eliminated the background signals from the
8 PDMS substrates (thickness ~ 4mm) by subtracting the absorbance of the PDMS substrate.
9

10 Figure panels 3b and c illustrate the transmittance spectra and the transmittance at $\lambda = 550$ nm
11 for the pristine Ag NW network film and Ni coated Ag NW network film, respectively. At
12 $\lambda = 550$ nm, the transmittance of the pristine Ag NW network film is 85.2 % but it gradually
13 decreases to lower transmittance by longer period of Ni electrodeposition. ($T_{\lambda=550\text{nm}} = 81.41,$
14 74.99, 48.66 and 37.01 % for samples A, B, C, and D) This is due to the increase of FF of the
15 Ag NW network film by the deposition of thicker Ni layers on the surface of Ag NWs.
16
17

18 The figure of merits (FoM) of TCEs, defined as the ratio of the electrical conductance and
19 the optical conductance ($\sigma_{\text{opt}}/\sigma_{\text{dc}}$) is calculated by commonly used equation as follows:^[28, 29]
20

$$21 \quad T = \left(1 + \frac{188.5 \sigma_{\text{opt}}}{R_s \sigma_{\text{dc}}} \right)^{-2}$$

22 where R_s is the sheet resistance and T is the transmission at 550nm, respectively. The FoM
23 of the pristine Ag NW network film is 72.62, while those of samples A, B, C and D are 60.04,
24 46.79, 20.62 and 29.51, respectively (Figure 3d). The decrease of FoMs for the Ni coated Ag
25 NW network is mainly due to the reduced transmittance. Furthermore, the FoM of the Ni
26 coated Ag NW network film with short deposition periods (5 and 20 seconds) meet the
27 minimum requirement of the industrial standard for ITO replacement as a transparent
28 conductive electrode (FoM > 36) suggested in the previous report.^[30] However, samples C
29 and D show lower values than this criterion. The mechanical robustness is also an important
30 factor for flexible and wearable electronic applications. To this end, we have conducted the
31
32
33
34
35
36
37
38
39
40
41
42
43
44
45
46
47
48
49
50
51
52
53
54
55
56
57
58
59
60
61
62
63
64
65

1 bending test for more than 1,000 bending/relaxation cycles from a flat ($\rho=\infty$) to bended ($\rho=1$
 2
 3
 4 cm) state. As shown in Figure 3f, the sheet resistances of the pristine Ag NW network and
 5
 6 sample C are slightly increased from 21.98 Ω/sq and 16.16 Ω/sq to 32.92 Ω/sq and 23.04 Ω/sq ,
 7
 8 respectively, by 1000 cycles of bending but show gradual saturation. This result verifying that
 9
 10 the Ni coated Ag NW network partially embedded on the substrate can be used as
 11
 12 mechanically robust transparent conductive electrodes for flexible electronic applications.
 13
 14

15
 16
 17 The formation of the core-shell structure of Ag NW and Ni shell layer enables protection of
 18
 19 the core Ag NWs from oxidative or corrosive environments. This could be confirmed by the
 20
 21 measurement of sheet resistance of the samples and x-ray photoelectron spectroscopy (XPS)
 22
 23 analysis before and after exposure to the chemically harsh environment (See Figure 4 and 6
 24
 25 for the electrical measurement, and Figure 5 and 7 for the XPS analysis). To evaluate the
 26
 27 corrosion resistance of the Ni coated Ag NW networks in the air, the change of electrical
 28
 29 resistance was measured under accelerated test (80 °C and 85 % of relative humidity (RH)).
 30
 31

32
 33 **Figure panels 4a and b** show the changes of the sheet resistance of the pristine Ag NW
 34
 35 network film and Ni coated Ag NW network film during the 80°C / 85% RH accelerated test.
 36
 37 After 12 hours of 80°C / 85% RH accelerated test, the sheet resistance of the pristine Ag NW
 38
 39 network film rapidly increased to 7.11 times ($R_s=36.16\Omega/\text{sq}$ to $R_s=256.93\Omega/\text{sq}$). On the other
 40
 41 hand, the sheet resistances of the samples A, B, C and D were slightly changed to 0.89, 1.35,
 42
 43 1.38 and 1.58 times, respectively. Furthermore, we conducted the 80°C / 85% RH accelerated
 44
 45 test for much longer periods. The sheet resistance of the pristine Ag NW network film was
 46
 47 increased to 7.17 times after 1 day, which continued to grow up to 15.46 times within 12 days.
 48
 49 However, it started to grow rapidly after 12 days, showing a dramatic raise up to 27.63 times
 50
 51 and 46.96 times after 13 and 14 days, respectively. On the contrary, the sheet resistances of
 52
 53 samples A, B, C and D were only slightly increased to 1.18, 1.48, 1.37 and 1.54 times,
 54
 55 respectively, after 14 days of 80°C / 85% RH accelerated test.
 56
 57
 58
 59
 60
 61
 62
 63
 64
 65

1 The surface morphologies of the pristine and Ni coated Ag NW network films after 80°C /
2
3 85% RH accelerated test were observed by scanning electron microscopy (SEM) analysis. For
4
5 all the samples, there are no significant changes on the morphology of the Ag NW network
6
7 films (Compare Figure panels 2a-e with Figure panels 4c-g). However, the XPS results verify
8
9 the change of material composition via chemical reaction. In **Figure 5**, the XPS spectra of the
10
11 pristine Ag NW network film (Figure panels 5a-c) and sample C (Figure panels 5d-g) before
12
13 and after the 80°C / 85% RH accelerated test are shown. The peak positions of the Ag 3d_{3/2}
14
15 and Ag 3d_{5/2} shifted from 374.23 eV to 374.70 eV and from 368.19 to 368.67 eV, respectively,
16
17 after 80°C / 85% RH accelerated test for the pristine Ag NW network film (Figure 5a). Here,
18
19 the increase of binding energy mainly stems from the sulfurization of Ag.^[19] In addition, the
20
21 sulfur (S) 2p peaks were observed after 80°C / 85% RH accelerated test (Figure 5b). The
22
23 sulfurization of Ag NW is caused by sulfur-containing gases such as carbonyl sulfide (OCS),
24
25 sulfur dioxide (SO₂) and carbon disulfide (CS₂), which is enhanced at higher relative
26
27 humidity^[31-33]. The O 1s peak for pristine Ag NW at 532.66 eV was observed, which shows
28
29 similar value with those of PDMS in the literature.^[34] This broad O 1s peak is attributed by
30
31 interaction between oxygen in the carboxyl group of the PVP chain on surface of the Ag
32
33 NWs^[19, 35] (Figure 5c). In contrast, the changes of Ag 3d peak positions (368.17 eV → 368.40
34
35 eV for Ag 3d_{3/2} and 374.14 → 374.38 eV for Ag 3d_{5/2}) for the sample C are smaller than those
36
37 for the pristine Ag NW network film, which confirms better resistance against sulfurization
38
39 by the Ni layer electroplated on the Ag NWs. Moreover, the sample C shows little changes of
40
41 Ni peaks (Figure 5g) after the 80°C / 85% RH accelerated test. According to our XPS spectra
42
43 measurements, the Ag NW network film coated with the Ni layer is less sulfurized than the
44
45 pristine Ag NW network after the 80°C / 85% RH accelerated test. For the Ag NW network
46
47 film coated with the Ni layer for short periods (5-20 seconds), NWs are only partially covered
48
49 with Ni layer and considerable portion of Ag NWs are exposed to the environment. In this
50
51
52
53
54
55
56
57
58
59
60
61
62
63
64
65

1 case, the anti-sulfurization effect of the Ni layer could be explained by reactive series of
 2
 3 metals^[36] and galvanic corrosion.^[37] During the exposure, the coated Ni film and Ag NWs act
 4
 5 as cathode and anode in the galvanic cell, respectively, since the standard electromotive force
 6
 7 of Ni ($V_{sce}=-0.799$ V) is much lower than that of Ag ($V_{sce}=0.257$ V). When both materials are
 8
 9 exposed to corrosive environment, the cathodic protection layer (Ni) donates electrons to Ag
 10
 11 NWs so that it prevents the corrosion of Ag NWs. On the other hand, after electrodeposition
 12
 13 for longer periods (50-100 seconds, sample C and D), Ag NWs are fully covered with a Ni
 14
 15 shell layer. In this case, the Ni shell forbids Ag NWs from a direct contact to sulfur. Therefore,
 16
 17 in this case, physical barrier against the sulfurization reaction and diffusion by the Ni layer as
 18
 19 well as its electron donation prohibit the sulfurization of the Ag NW network film and prevent
 20
 21 the decrease of electrical conductance.
 22
 23
 24
 25
 26

27 The chemical stability of the Ni coated Ag NW network film against sulfurization and
 28
 29 oxidation was characterized by measuring the electrical resistance of the samples during Na₂S
 30
 31 solution exposure (i.e. 5 wt% of Na₂S in DI water). **Figure 6a** presents the changes of the
 32
 33 sheet resistance for the pristine and Ni coated Ag NW network films after the immersion in
 34
 35 Na₂S solution. The sheet resistance of the pristine Ag NW network film is drastically
 36
 37 increased by 113.83 times (15.90 Ω/sq → 1810.00 Ω/sq) only after 21 seconds. The sample A
 38
 39 and B also exhibit a rapid corrosion by Na₂S solution with a dramatic increase of the electrical
 40
 41 resistance. However, the sample C and D present a tremendous enhancement of chemical
 42
 43 resistance against corrosion, which is verified by much smaller changes of electrical
 44
 45 resistances (i.e. 6.44 and 8.48 times increase of the sheet resistance for the samples C and D
 46
 47 after 300 seconds in the Na₂S solution). As shown in Figure 6b, the pristine Ag NWs are
 48
 49 broken into small pieces due to the corrosion. Thin Ni layers on the Ag NWs could not protect
 50
 51 them from sulfurization and oxidation reaction as shown in Figure panels 6c-d for the samples
 52
 53 A and B. However, the samples C and D exhibit the preservation of structural integrity
 54
 55
 56
 57
 58
 59
 60
 61
 62
 63
 64
 65

1 without any fracture or damage on the surface (Figure 6e-f). After the sulfurization reaction, a
 2
 3 few cubic crystallites of Ag₂S are observed on the Ag NW network film (Figure 6f). The XPS
 4
 5 results for the pristine Ag NW network film before and after the reaction with the Na₂S
 6
 7 solution are shown in **Figure 7a-c**. When Ag NW reacted with Na₂S solution, wider spectrum
 8
 9 of Ag 3d, O1s with several small peaks and S 2p peaks were observed (Figure 7a-c). Here, the
 10
 11 wide Ag 3d spectrum can be deconvoluted into the six peaks ($E_B=369.30$ eV, 364.90 eV and
 12
 13 368.11 eV for Ag 3d_{5/2} and $E_B=375.40$ eV, 374.32 eV and 373.00 eV for Ag 3d_{3/2}) as shown in
 14
 15 Figure 7a. $E_B=369.30$ eV (Ag 3d_{5/2}) and $E_B=375.40$ eV (Ag 3d_{3/2}) of sample C are higher than
 16
 17 those of the pristine Ag NW (368.19 eV and 374.23 eV for Ag 3d_{5/2} and Ag 3d_{3/2},
 18
 19 respectively) due to the sulfurization of Ag NW by H₂S existing in the Na₂S solution.^[19] The
 20
 21 lower binding energies $E_B= 364.90$ eV and 368.11 eV (Ag 3d_{5/2}) and $E_B=373.00$ eV and 374.32
 22
 23 eV (Ag 3d_{3/2}) indicate the formation of Ag₂O by the absorption and reaction with oxygen
 24
 25 species such as OH⁻ ion^[38] and O₂^[39] within the Na₂S solution. The oxidation of Ag can also
 26
 27 be confirmed by the deconvoluted lower peaks at 529.40 eV and 530.70 eV for O1s (Figure
 28
 29 7c)^[40, 41]. In contrast, the sample C presents much smaller change of the peak positions of Ag
 30
 31 3d_{3/2} due to much less formation of Ag₂S in the sample C than in the pristine Ag NW (Figure
 32
 33 7d). The peak position of Ni 2p_{3/2} is slightly shifted due to small sulfurization of Ni shell.
 34
 35 Higher satellite peaks at 855.50 eV for Ni 2p_{3/2} and 872.90 eV for Ni 2p_{5/2} are caused by the
 36
 37 oxidation of Ni^[42] with oxygen species in the Na₂S solution. In summary, we can confirm that
 38
 39 Ag NW network film is protected from the severe sulfurization and oxidation by the Ni shell
 40
 41 layer in spite of its minor corrosion.

42 The anti-corrosion mechanism of Ag NWs by the thick Ni shell layer (samples C and D)
 43
 44 can be explained by the galvanic corrosion and thermodynamic effect. The electrode potential
 45
 46 difference of Ni and Ag induces cathodic protection of Ag NWs by the Ni shell layer,
 47
 48 resulting in the delay of galvanic corrosion such as oxidation and sulfurization of Ag NWs. In
 49
 50

1 addition, the Ni shell layer can reduce the sulfurization of the core Ag NW structure due to
2
3 the resistance of Ni against the sulfurization reaction. The Gibbs free energy (ΔG) for the
4
5 formation of nickel sulfide (NiS) in Na₂S aqueous solution at room temperature is -119.7
6
7 kJ/mol, which is smaller than that value of silver sulfide (Ag₂S), -280.7 kJ/mol.^[43] Therefore,
8
9 the sulfurization of Ni shell layer is much slower than that of the core Ag NWs. As a result,
10
11 Ag NWs can be protected from the rapid sulfurization via the barrier effect of the Ni shell
12
13 layer.
14
15
16

17
18 We further illustrate the sulfurization and oxidation effects of the pristine Ag NW
19
20 network film and sample C by constructing a simple LED circuit (**Figure 8a**). Here the
21
22 pristine and Ni coated Ag NW network films were used as a conductor serially connected to
23
24 the LED lamp. As depicted in Figure 8b-d, the LED was turned off since the electrical
25
26 conductance of the pristine Ag NW network film was electrically nonconductive after 80°C /
27
28 85% RH accelerated test and Na₂S liquid-phase corrosion test. On the other hand, the
29
30 illumination intensity of LED lamp was not significantly degraded for sample C after 80°C /
31
32 85% RH accelerated test and Na₂S liquid-phase corrosion test (Figure 8e-g). This result
33
34 confirms that Ni coating on the Ag NW network maintains the functionality of the
35
36 interconnection in the circuit.
37
38
39
40
41
42
43
44

45 **3. Conclusions**

46
47 In summary, we have developed a novel method to improve the chemical stability of
48
49 the Ag NW network film based transparent conductive electrode simply by local
50
51 electrodeposition of Ni layer along the Ag NWs. We observed enhancement of the electrical
52
53 conductivity after electrodeposition of Ni layer on the Ag NW network film by the welding
54
55 effect. Furthermore, Ni coated Ag NW network films exhibit an excellent chemical resistance
56
57 against the oxidation as well as the sulfurization reaction compared with very large resistance
58
59 deviation of the pristine Ag NW network exposed to the harsh environment. Cathodic
60
61
62
63
64
65

1 protection and chemical resistance of Ni shell layer prevent the oxidation and sulfurization of
 2
 3 the core Ag NWs. Therefore, this method can maintain the performance of devices without
 4
 5 degradation. We believe that our proposed method can be applicable to the chemical
 6
 7 protection of a variety of conductive nanomaterial based electrodes. Especially, this method
 8
 9 will be extremely useful for the applications in which conductive nanomaterial electrodes are
 10
 11 directly exposed to the harsh environment or immersed in chemically reactive liquids.
 12
 13 Moreover, the applications can be further extended to toxic chemical sensing in harsh
 14
 15 environment.
 16
 17
 18
 19
 20
 21

22 **4. Experimental Section**

23 Ag NWs were synthesized by the polyol method according to the literature.¹⁴ First,
 24
 25 5.86 g of polyvinylpyrrolidone (PVP) in 190 ml of glycerol was heated at 55 °C. Then, 0.059
 26
 27 g of NaCl, 0.5 ml of DI water and 1.58 g of AgNO₃ were poured into the preheated mixture.
 28
 29 The solution was heated up to 155 °C within 10 min with gentle stirring. Finally, the solution
 30
 31 was filtered by vacuum filtration method and Ag NWs were stored in diluted methanol for
 32
 33 further experiments.
 34
 35
 36
 37

38 Ni layer was electrodeposited on the exposed surface of the Ag NW network film.
 39
 40 Here, a Ni electrodeposition bath consisting of 1 M nickel sulfate hexahydrate
 41
 42 (NiSO₄·6H₂O), 0.2M nickel chloride hexahydrate (NiCl₂·6H₂O) and 0.5M boric acid (H₃BO₃)
 43
 44 in DI water was used. A three electrode cell configuration including Ag NW network film
 45
 46 buried on the PDMS film as a working electrode, platinum (Pt) coated titanium (Ti) plate as
 47
 48 an insoluble counter electrode, and Ag/AgCl (saturated KCl) electrode as a reference
 49
 50 electrode was used at a room temperature condition with a stirring rate of 200 rpm. The Ag
 51
 52 NW network film buried on the surface of PDMS was electrically connected with aluminum
 53
 54 plate by painting the silver paste at the edge of Ag NW network film and passivated by
 55
 56 painting a commercial manicure except the working area (exposed area = 15 x 15 mm²) for
 57
 58
 59
 60
 61
 62
 63
 64
 65

1 electrodeposition. A constant potential of -0.9 V was applied for various electrodeposition
2
3 periods (0-100 seconds) by using a potentiostat/galvanostat (601D, CH Instruments, Inc.).
4

5
6 The surface morphologies of the samples were investigated by using a scanning
7
8 electron microscope (SEM, Sirion FE-SEM, FEI) and composition of the samples were
9
10 determined by energy dispersive spectroscopy (EDS). Also, the chemical compositions and
11
12 crystallographic structures of the Ag NW network and Ni coated Ag NW network were
13
14 studied by XPS (Sigma Probe, Thermo VG Scientific, Inc.) and X-ray diffraction (Rigaku
15
16 D/max-2500) using a Cu K α radiation ($\lambda=1.5405 \text{ \AA}$) at 40 kV and 300 mA.
17
18
19
20
21
22
23
24

25 **Acknowledgements**

26
27 This research was supported by the grants from the Basic Science Research Program
28
29 (2013006809) and Global Frontier R&D Program (2011-0031563) funded by the National
30
31 Research Foundation (NRF) and from KIMM (Korea Institute of Machinery & Materials)
32
33 Research (SC0940) under the Ministry of Science, ICT and Future Planning of Korea. This
34
35 work was also financially supported by the Graphene Materials and Components
36
37 Development Program of MOTIE/KEIT (10044412).
38
39
40
41
42
43
44
45
46

47 [1] H. Schmidt, H. Flugge, T. Winkler, T. Bulow, T. Riedl, W. Kowalsky, Appl Phys Lett
48
49 2009, 94.

50
51 [2] J. P. B. Mark J. Pellerite, Marie A. Boulos, Patrick M. Campbell,, A. J. H. Eileen M.
52
53 Haus, Manoj Nirmal, Marc D. Radcliffe, Ralph R. Roberts,, J. K. W. John J. Stradinger, Brian
54
55 T. Weber In 14.2: New Transparent Electrodes for Cholesteric Liquid Crystal Displays, SID
56
57
58
59
60
61
62
63
64
65

Symposium Digest of Technical Papers, SID Symposium Digest of Technical Papers: 2012;

172.

[3] S.-Y. R. Kwan Hee Lee, Jang Hyuk Kwon, Sang Wook Kim, Ho Kyoong Chung In 9.3:

2.2” QCIF Full Color Transparent AMOLED Display, SID Symposium Digest of Technical Papers, 2012; 2003; 4.

[4] D. S. Hecht, L. B. Hu, G. Irvin, *Adv Mater* 2011, 23, 1482.

[5] C. Peng, Z. Jia, H. Neilson, T. Li, J. Lou, *Adv Eng Mater* 2013, 15, 250.

[6] L. B. Hu, H. S. Kim, J. Y. Lee, P. Peumans, Y. Cui, *Acs Nano* 2010, 4, 2955.

[7] S. Kim, J. Yim, X. Wang, D. D. C. Bradley, S. Lee, J. C. Demello, *Adv Funct Mater* 2010, 20, 2310.

[8] S. Bae, H. Kim, Y. Lee, X. F. Xu, J. S. Park, Y. Zheng, J. Balakrishnan, T. Lei, H. R. Kim, Y. I. Song, Y. J. Kim, K. S. Kim, B. Ozyilmaz, J. H. Ahn, B. H. Hong, S. Iijima, *Nat Nanotechnol* 2010, 5, 574.

[9] C. Celle, C. Mayousse, E. Moreau, H. Basti, A. Carella, J. P. Simonato, *Nano Res* 2012, 5, 427.

[10] C. H. Liu, X. Yu, *Nanoscale Res Lett* 2011, 6.

[11] Y. G. Sun, Y. N. Xia, *Adv Mater* 2002, 14, 833.

[12] K. E. Korte, S. E. Skrabalak, Y. N. Xia, *J Mater Chem* 2008, 18, 437.

[13] Y. G. Sun, B. Mayers, T. Herricks, Y. N. Xia, *Nano Lett* 2003, 3, 955.

[14] J. Lee, I. Lee, T. S. Kim, J. Y. Lee, *Small* 2013, 9, 2887.

[15] C. H. Chung, T. B. Song, B. Bob, R. Zhu, Y. Yang, *Nano Res* 2012, 5, 805.

[16] V. Scardaci, R. Coull, P. E. Lyons, D. Rickard, J. N. Coleman, *Small* 2011, 7, 2621.

[17] D. Kim, L. J. Zhu, D. J. Jeong, K. Chun, Y. Y. Bang, S. R. Kim, J. H. Kim, S. K. Oh, *Carbon* 2013, 63, 530.

[18] H. H. Khaligh, I. A. Goldthorpe, *Nanoscale Res Lett* 2013, 8.

- 1 [19] J. L. Elechiguerra, L. Larios-Lopez, C. Liu, D. Garcia-Gutierrez, A. Camacho-
2
3 Bragado, M. J. Yacaman, Chem Mater 2005, *17*, 6042.
4
5 [20] H. Aziz, Z. Popovic, C. P. Tripp, N. X. Hu, A. M. Hor, G. Xu, Appl Phys Lett 1998,
6
7 72, 2642.
8
9 [21] J. A. Craig Hillman, Seth Binfield In SILVER AND SULFUR: CASE STUDIES,
10
11 PHYSICS, AND POSSIBLE SOLUTIONS, SMTA International 2007; 13.
12
13 [22] A. K. N. Chawdhury, M. G. Harrison, D. H. Hwang, A. B. Holmes, and R. H. Friend,
14
15 Synthetic Metals 1999, *102*, 2.
16
17 [23] J. Liang, L. Li, K. Tong, Z. Ren, W. Hu, X. Niu, Y. Chen, Q. Pei, Acs Nano 2014, *8*,
18
19 1590.
20
21 [24] X. Y. Zeng, Q. K. Zhang, R. M. Yu, C. Z. Lu, Adv Mater 2010, *22*, 4484.
22
23 [25] A. R. Rathmell, M. Nguyen, M. F. Chi, B. J. Wiley, Nano Lett 2012, *12*, 3193.
24
25 [26] Y. Tao, Y. X. Tao, L. Y. Wang, B. B. Wang, Z. G. Yang, Y. L. Tai, Nanoscale Res
26
27 Lett 2013, *8*.
28
29 [27] M. Paunovic, M. Schlesinger, in *Fundamentals of electrochemical deposition*, Vol.,
30
31 Wiley-Interscience, 2nd ed.; Hoboken, N.J. 2006; Ch. 11
32
33 [28] S. De, T. M. Higgins, P. E. Lyons, E. M. Doherty, P. N. Nirmalraj, W. J. Blau, J. J.
34
35 Boland, J. N. Coleman, Acs Nano 2009, *3*, 1767.
36
37 [29] J. V. van de Groep, P. Spinelli, A. Polman, Nano Lett 2012, *12*, 3138.
38
39 [30] S. De, J. N. Coleman, Acs Nano 2010, *4*, 2713.
40
41 [31] R. L. P. H. E. Bennett, D. K. Burge, and J. M. Bennett, Journal of Applied Physics
42
43 1969, *40*, 11.
44
45 [32] T. E. Graedel, J. P. Franey, G. J. Gualtieri, G. W. Kammlott, D. L. Malm, Corros Sci
46
47 1985, *25*, 1163.
48
49 [33] T. E. Graedel, J Electrochem Soc 1992, *139*, 1963.
50
51
52
53
54
55
56
57
58
59
60
61
62
63
64
65

- 1 [34] P. Holgerson, D. S. Sutherland, B. Kasemo, D. Chakarov, *Appl Phys a-Mater* 2005, *81*,
 2
 3 51.
 4
 5 [35] C. W. Xiao, H. T. Yang, C. M. Shen, Z. A. Li, H. R. Zhang, F. Liu, T. Z. Yang, S. T.
 6
 7 Chen, H. J. Gao, *Chinese Phys* 2005, *14*, 2269.
 8
 9 [36] J. E. Brady, G. E. Humiston, in *General chemistry, principles and structure*, Vol.,
 10
 11 Wiley, 3rd ed.; New York 1982; Ch. chapter
 12
 13 [37] R. W. Revie, H. H. Uhlig, in *Uhlig's corrosion handbook*, Vol., Wiley, 3rd ed.;
 14
 15 Hoboken, N.J. 2011; Ch. chapter
 16
 17 [38] X. Bao, M. Muhler, B. Pettinger, Y. Uchida, G. Lehmpfuhl, R. Schlogl, G. Ertl, *Catal*
 18
 19 *Lett* 1995, *32*, 171.
 20
 21 [39] J. Y. Liu, K. G. Pennell, R. H. Hurt, *Environ Sci Technol* 2011, *45*, 7345.
 22
 23 [40] E. R. Savinova, D. Zemlyanov, B. Pettinger, A. Scheybal, R. Schlogl, K. Doblhofer,
 24
 25 *Electrochim Acta* 2000, *46*, 175.
 26
 27 [41] Y. Abe, T. Hasegawa, M. Kawamura, K. Sasaki, *Vacuum* 2004, *76*, 1.
 28
 29 [42] D. L. Legrand, H. W. Nesbitt, G. M. Bancroft, *Am Mineral* 1998, *83*, 1256.
 30
 31 [43] P. Y. Fuxiang Huang, Yonghong Xu, and Ying Zhang In *Study on Microstructure and*
 32
 33 *Corrosion Behavior of Ag-Cu-Zn-Ni Alloys*, Advanced Materials Research, *Switzerland*,
 34
 35 Trans Tech Publications: *Switzerland*, 2011; 2132.
 36
 37
 38
 39
 40
 41
 42
 43
 44
 45
 46
 47

48 Received: ((will be filled in by the editorial staff))

49 Revised: ((will be filled in by the editorial staff))

50 Published online on ((will be filled in by the editorial staff))

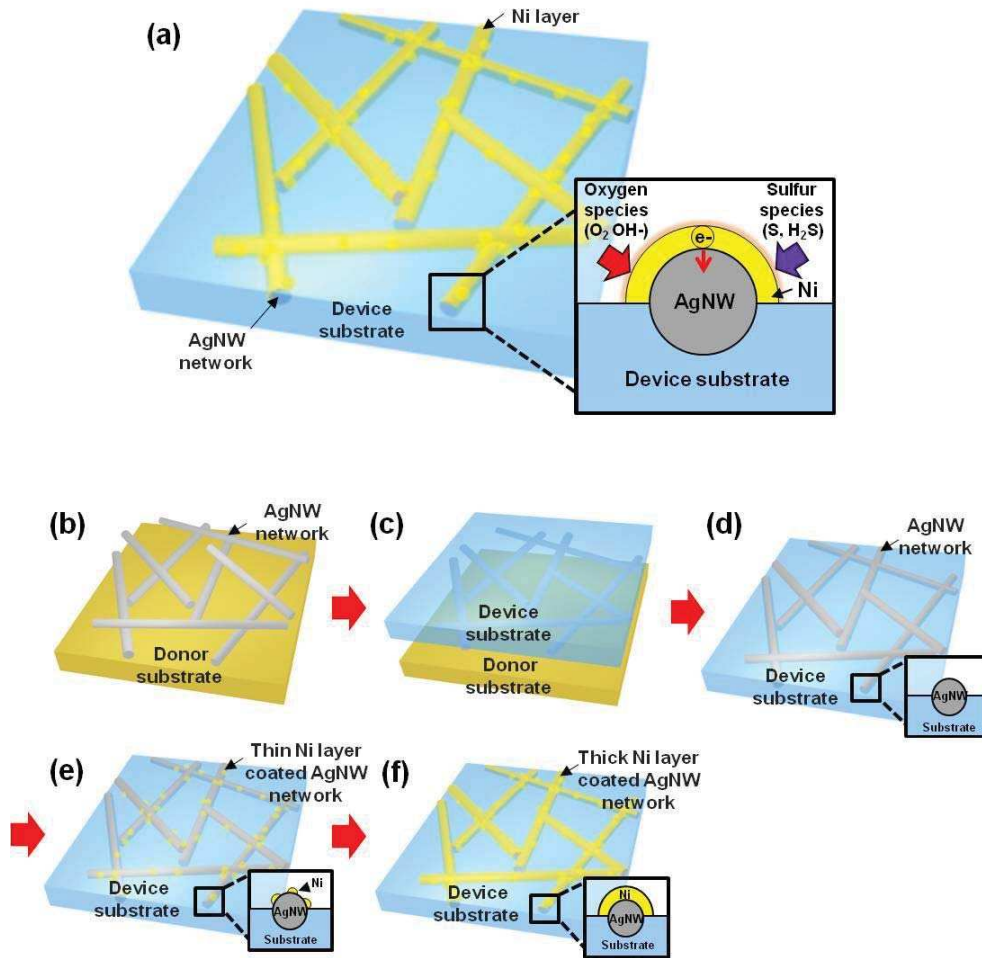


Figure 1. Mechanism and fabrication process: (a) illustration of the Ni coated Ag NW network film, (inset) schematic of anti-oxidation and anti-sulfurization mechanisms of the Ni layer on the surface of Ag NW network; (b-f) fabrication process for the Ni coated Ag NW network film ((b) formation of the Ag NW network on donor substrate by spray coating, (c) formation of buried Ag NW network film on the device substrate (here, uncured PDMS film is poured and thermally cured), (d) the Ag NW network film partially embedded on the surface of device substrate, (e) nucleation of the thin Ni layer on the Ag NW network film by electrodeposition and (f) formation of the thick Ni layer by longer electrodeposition on the Ag NW network film.

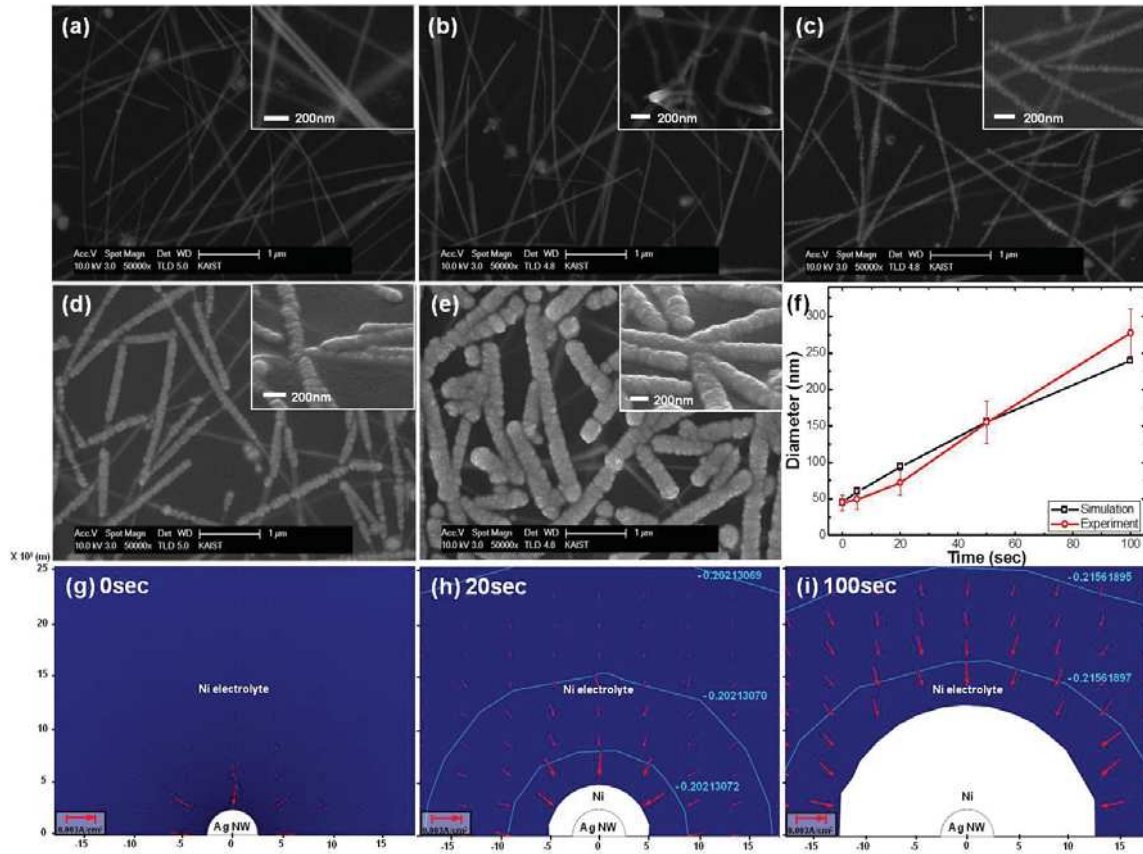


Figure 2. The surface SEM images of the Ag NW network film: (a) pristine Ag NWs, (b) sample A, (c) B, (d) C, and (e) D; Ag NWs coated with Ni layer for various electrodeposition periods (0 seconds (a), 5 seconds (b), 20 seconds (c), 50 seconds (d) and 100 seconds (e)); (f) measured and simulated diameters of Ag@Ni core-shell NWs; (g-i) cross-sectional image of single Ag@Ni core-shell NW after different electrodeposition periods (g-i: 0, 20 and 100 seconds) obtained by numerical simulation. In this case, Ag NW was embedded in the substrate by 50 % in area.

Table 1. Physical parameter changes of the Ag NW network film by the electrodeposition of Ni layer: average diameter, fill factor (FF), transmittance at 550nm wavelength, and the sheet resistance

Sample name	Pristine Ag NW network film	A	B	C	D
Period of Ni electrodeposition (sec)	0	5	20	50	100
Diameter (nm)	45.05 (± 10.67)	49.23 (± 14.33)	72.33 (± 17.12)	154.85 (± 29.14)	277.60 (± 32.88)
FF (%)	23.39	23.99	29.34	34.16	66.32
T _{550nm} (%)	85.27	81.41	74.99	48.66	37.01
R _s (Ω /sq)	31.07 (± 3.56)	28.98 (± 7.74)	26.03 (± 7.92)	21.09 (± 5.88)	9.92 (± 5.42)

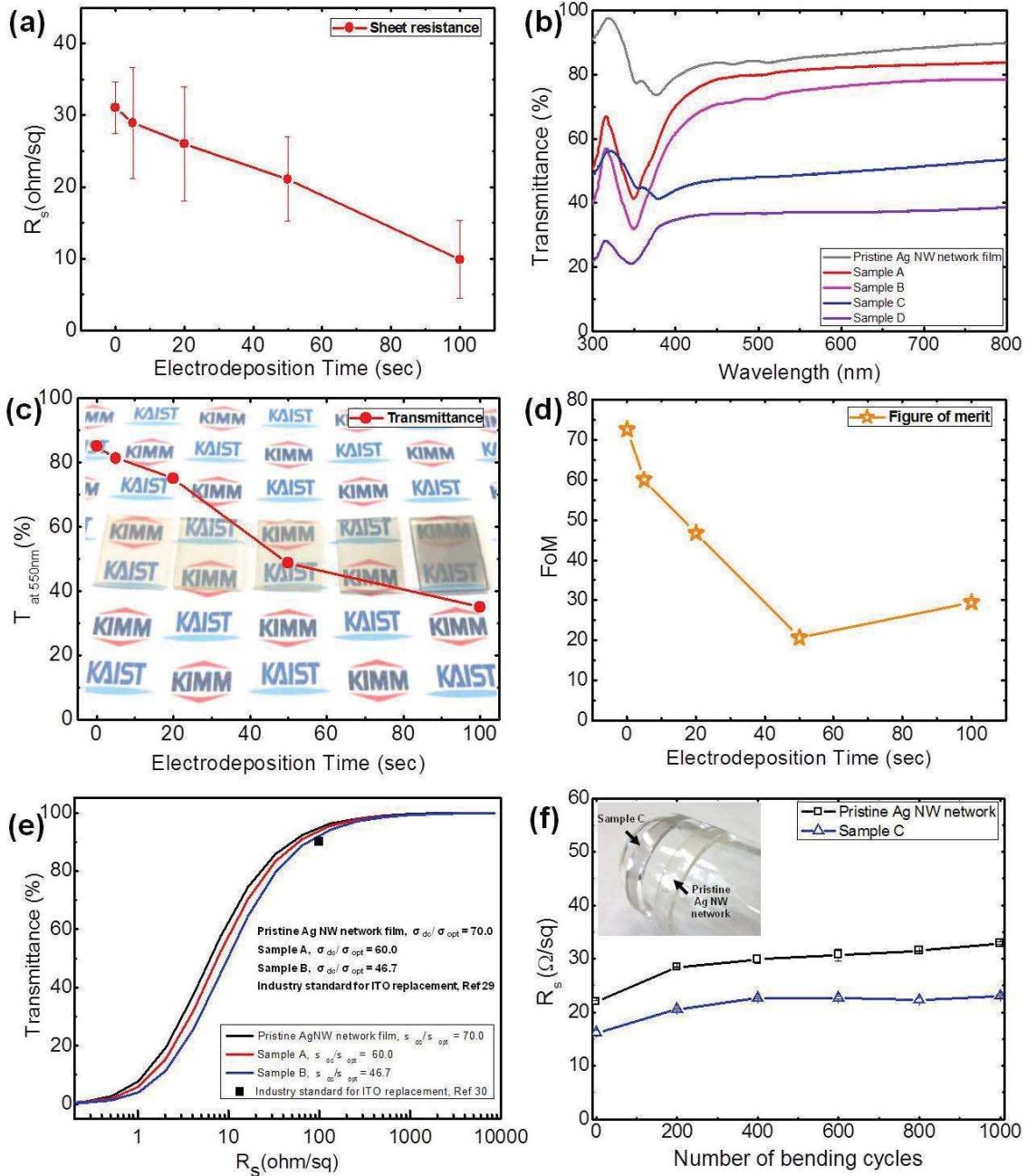


Figure 3. Physical parameter changes of the Ag NW network film by the electrodeposition of Ni layer: (a) sheet resistance, (b) transmittance spectra and (c) transmittance at $\lambda = 550$ nm (d) figure of merit (FoM) and (e) transmittance vs. sheet resistance plot of Ag NWs embedded on PDMS, Ni-coated Ag NW network films (5, 20 sec), and the minimum industrial standard opto-electrical performance as an ITO replacement (black square) (f) Sheet resistance changes for the pristine Ag NW network and Sample C under cyclic bending/relaxation.

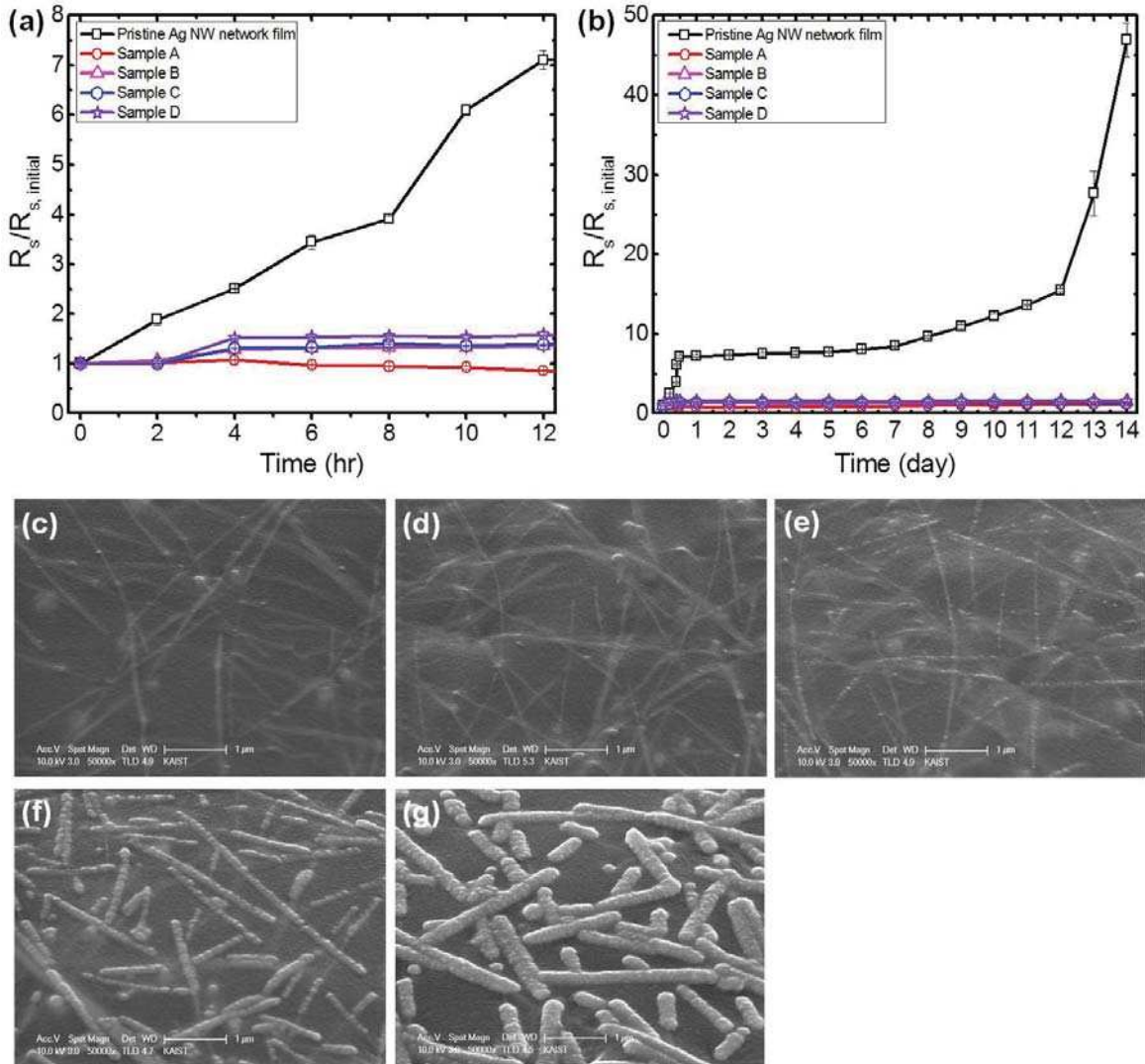


Figure 4. UV-Vis absorption measurement in transverse magnetic (TM) mode of fabricated nanostructure arrays: (a) A0 NW array, A45 NW array, and A60 NW array; (b) A0/gel NW array, A45/gel NW array, A60/gel NW array, Black dotted lines for each sub-figure represent non-polarized absorption of (a) Ag thin film and (b) Ag/gel-TiO₂ dual layer thin film, respectively.

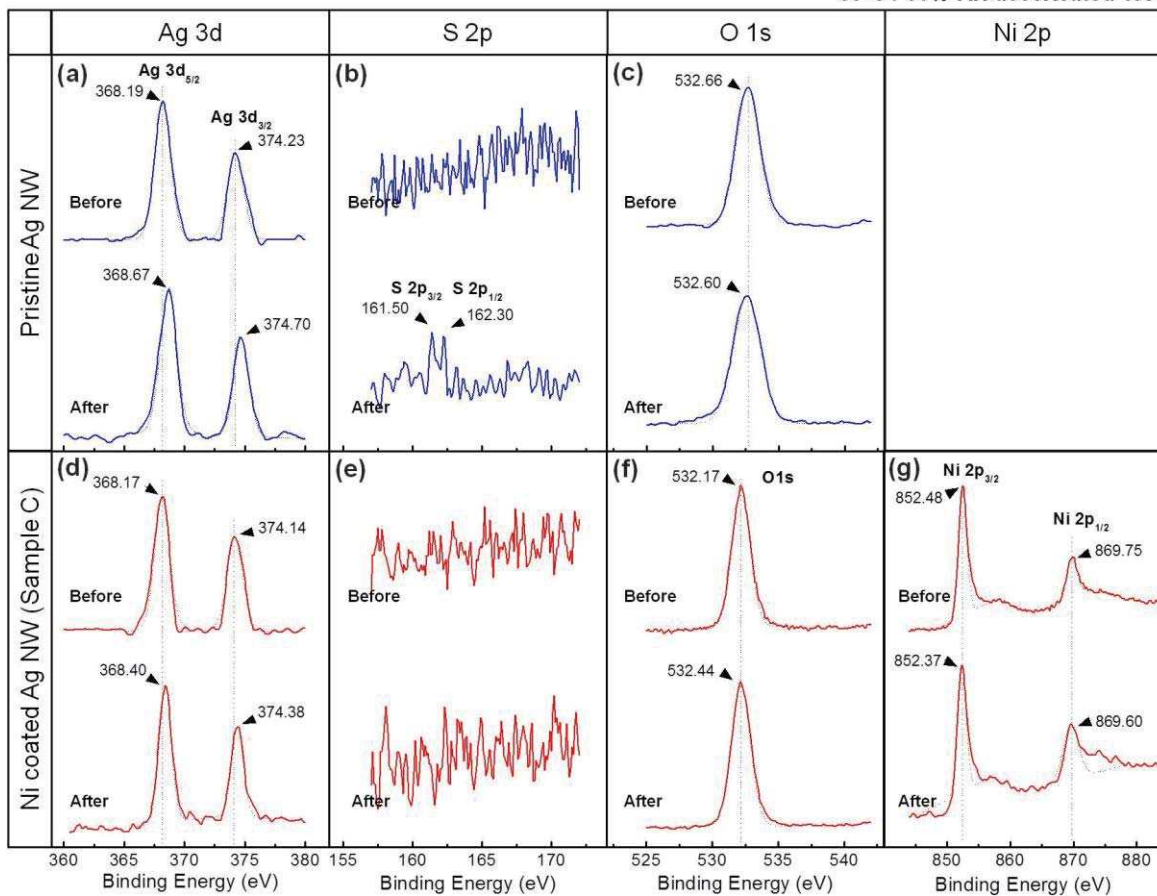


Figure 5. Change of XPS spectra for the pristine Ag NW network film and sample C by 80°C / 85% RH accelerated test: (a) Ag 3d spectra, (b) S 2p spectra, (c) O 1s spectra of the pristine Ag NW network film before and after 80°C / 85% RH accelerated test; (d) Ag 3d spectra, (e) S 2p spectra, (f) O 1s spectra and (g) Ni 2p spectra of the sample C before and after 80°C / 85% RH accelerated test.

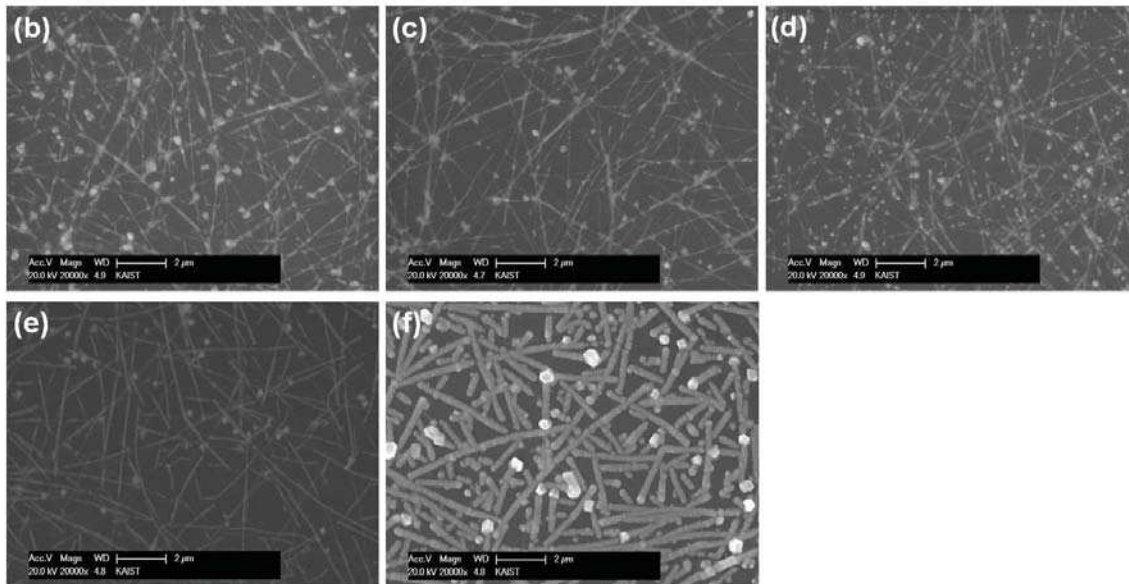
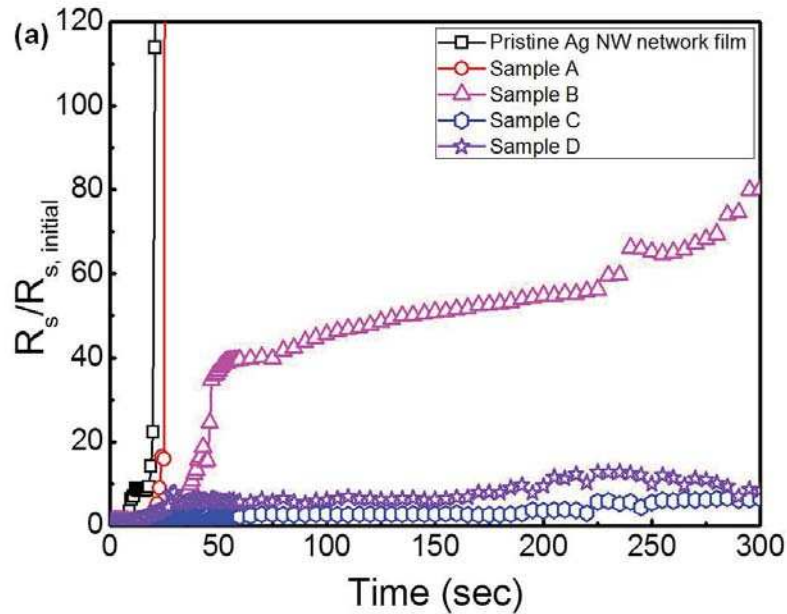


Figure 6. Effect of the Ni coating on the corrosion resistance of the Ag NW network film in Na_2S liquid-phase corrosion test: (a) Sheet resistance changes for the pristine and Ni coated Ag NW network film by exposure to the Na_2S solution for 300sec. SEM images of the pristine Ag NW network film (b) and sample A (c), B (d), C (e) and D (f) after immersing into the Na_2S solution for 300 seconds.

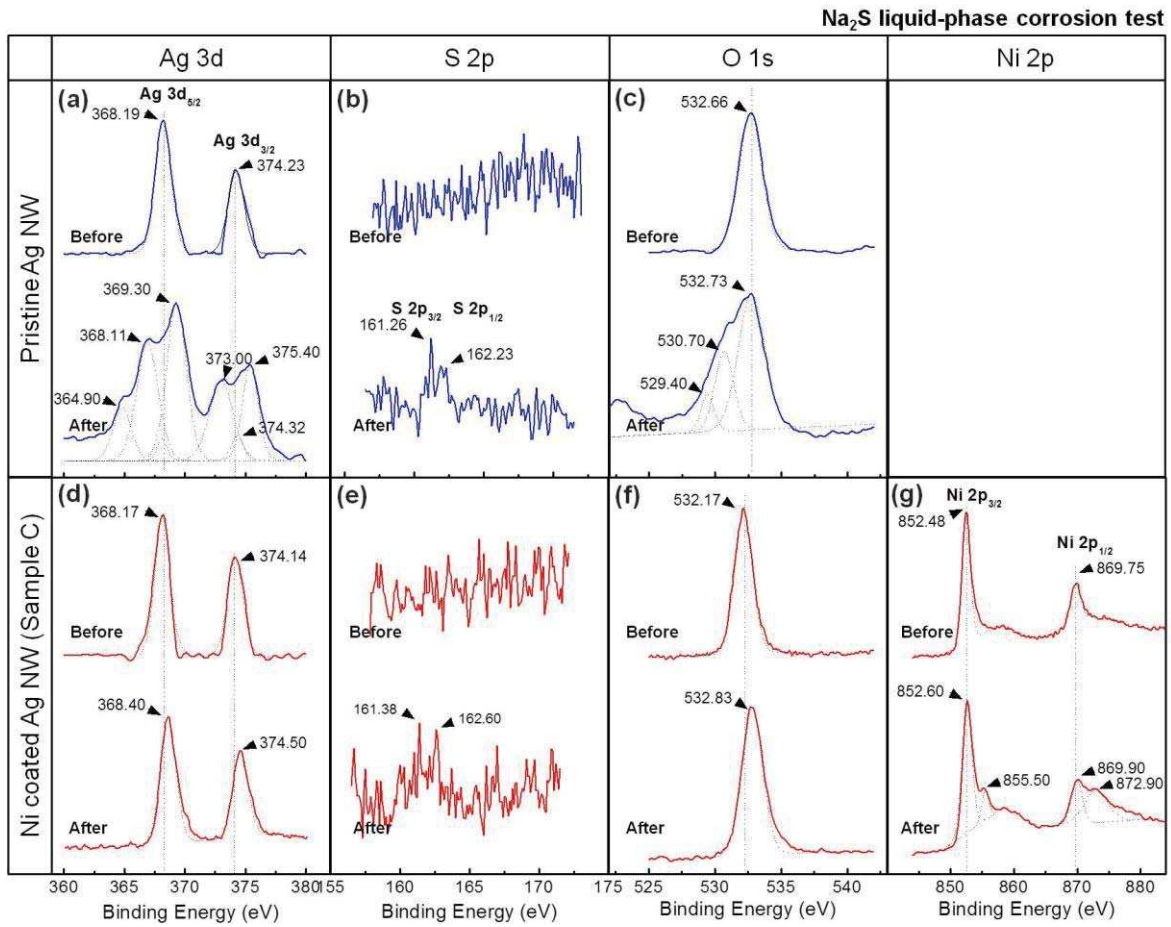


Figure 7. Change of XPS spectra for the pristine Ag NW network film and sample C by Na₂S liquid-phase corrosion test: (a) Ag 3d spectra, (b) S 2p spectra, (c) O 1s spectra of the pristine Ag NW network film before and after Na₂S liquid-phase corrosion test; (d) Ag 3d spectrum, (e) S 2p spectrum, (f) O 1s spectrum and (g) Ni 2p spectrum of the sample C before and after Na₂S liquid-phase corrosion test

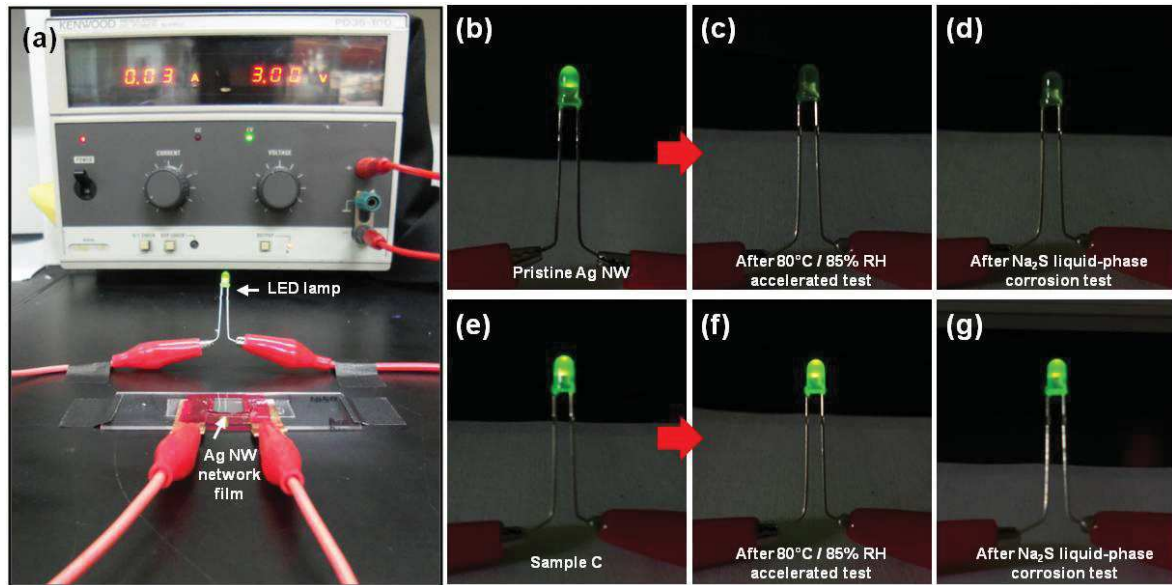


Figure 8. Corrosion effect of the Ag NW network based interconductor in the electrical circuit: (a) Photograph of the electrical circuit; LED is connected to the power source via Ag NW network based conductor. Illumination of LED connected via a pristine Ag NW network film before (b), after 80°C / 85% RH accelerated test (c) and after Na₂S liquid-phase corrosion test (d); Photograph of LED lamp using sample C as a connector; before (e), after 80°C / 85% RH accelerated test (f) and after Na₂S liquid-phase corrosion test (g)

The table of contents entry

The formation of Ag@Ni core-shell nanowire network film by partial embedding of Ag nanowires and local electrodeposition of Ni shell layer enhances the chemical resistance of the Ag nanowire network film based transparent electrode against oxidation and sulfurization. The mechanism can be explained by physical barrier against chemical reaction and diffusion as well as the prevention of galvanic corrosion via electron donation. This method provides very simple and facile route to the protection of transparent conductive electrode materials.

TOC Keyword

Transparent electrode, silver nanowire, electrodeposition, anti-oxidation, anti-sulfurization and core-shell nanostructure

H. Eom, J. Lee, A. Pichitpajongkit, M. Amjadi, J.H. Jeong, E. Lee, J.Y. Lee, and I. Park*

Electrodeposited Ni shell for the enhanced chemical stability of silver nanowire network

